Eur. Phys. J. D (2012) 66: 31
DOI: 10.1140/epjd/e2011-20663-4

THE EUROPEAN PHYSICAL JOURNAL D

Regular Article

Electron collisions with the BeH^+ molecular ion in the R-matrix approach

K. Chakrabarti[1] and J. Tennyson[2,a]

[1] Department of Mathematics, Scottish Church College, 1 & 3 Urquhart Sq., 700006 Kolkata, India
[2] Department of Physics and Astronomy, University College London, Gower St., WC1E 6BT London, UK

Received 13 November 2011 / Received in final form 20 December 2011
Published online 31 January 2012 –

Abstract. The R-matrix method is used to study electron collisions with the BeH^+ molecular ion. The diatomic version of the UK Molecular R-matrix codes is used and a configuration-interaction calculation is first performed for the BeH^+ target to obtain its potential energy curves for 19 lowest singlet and triplet states. Scattering calculations are then done to yield excitation and rotational excitation cross sections in the energy range 0−14 eV. Additionally we also obtain bound states of BeH and their quantum defects at the BeH equilibrium bond length $2.5369a_0$. Resonance positions and widths for Feshbach resonances in the e-BeH^+ system are also obtained and presented at the equilibrium bond length $2.5369a_0$.

1 Introduction

There is huge interest and potential environmental benefits in commercially viable reactors operating on fusion principles. Fusion experiments are already underway at the JET (joint European Torus) and several other places and will pave the way for ITER (international thermonuclear energy reactor), which is an experimental, commercially viable fusion reactor still under construction.

The difficulty with fusion reactors is their high operating temperatures and this makes it necessary to choose carefully, suitable wall material for the parts of the machine which face the hot plasma. Particularly important is the Divertor, a part of the machine that directly faces the hot plasma and extracts the heat and the helium ash and should withstand temperatures of about 3000 °C. The excellent thermal conductivity and low erosion of beryllium (Be) makes it a good choice for the Divertor walls, and its reliability is being actively tested in the JET fusion experiment [1] with a view to using beryllium as the walls in the new ITER. Since the plasma would contain H^+ ions, the use of Be as wall material indicates that the plasma would interact with the wall to form beryllium hydrides and, BeH^+ in particular as one of the components. The interaction of the electrons in the plasma with BeH^+ therefore needs to be understood and this motivates the present paper.

As a starting point, one needs a good representation of the target BeH^+ ion. Several good quality structure calculations of the BeH^+ molecule have been undertaken in the past. Ornellas [2] computed the potential energy (PE) curves and spectroscopic constants for the X $^1\Sigma^+$ and A $^1\Pi$ states of the BeH^+ molecule using a 1322-term configuration interaction (CI) wave function. Bishop and Cheung [3] also studied the X $^1\Sigma^+$ and A $^1\Pi$ states of BeH^+ using a 330-term CI wave function and reported results that were better than Ornellas [2] for the A$^1\Pi$ state. An improved calculation of the A $^1\Sigma^+$ was again undertaken by Ornellas [4] where, in addition to the PE curve, the dipole moment for this state as a function of geometry was also presented. A more complete study on the low lying states of BeH^+ was reported by Machado and Ornellas [5] at the multi reference singles and doubles configuration interaction (MRSDCI) level. For all these states, dipole moments and transition moments were computed. For the bound states, besides the vibrational levels, transition probabilities, radiative lifetimes, vibrationally-averaged dipole moments, and a set of spectroscopic constants were also reported.

To the best of our knowledge there is no previous work on electron impact cross section for the BeH^+ ion. In this work we present cross sections for electron collisions with BeH^+ considering their importance in the divertor plasmas in fusion devices. In addition, we present, at a single geometry, the bound states of BeH, their quantum defects and resonance parameters for Feshbach resonances in the e-BeH^+ system.

2 Calculations

2.1 Method

Our calculations use the R-matrix method [6]; a detailed discussion of its application for molecules can be found in a

[a] e-mail: j.tennyson@ucl.ac.uk

recent review [7]. The R-matrix method starts by dividing the configuration space into two regions, an inner region defined by a sphere, here of radius $11a_0$, centered at the molecular center of mass. This sphere encloses the entire N-electron target BeH^+ ion. In this inner region, the wave function of the $(N+1)$-electron system (BeH^+ + electron) is given by

$$\Psi_k = \mathcal{A}\sum_{i,j} a_{i,j,k}\Phi_i(1,\ldots,N)F_{i,j}(N+1) + \sum_i b_{i,k}\chi_i(1,\ldots,N+1), \quad (1)$$

where $\mathcal{A}$ is the antisymmetrisation operator, $F_{i,j}$ are continuum orbitals and χ_i are two-center L^2 functions constructed from N-electron target orbitals. The L^2 functions allow for polarization of the N-electron target wave function in presence of the projectile electron.

In equation (1), Φ_i is the wave function of the ith target state. Electron-correlation effects are included in these target wave functions via configuration interaction (CI) expansions. As discussed extensively in [8], the choice of this CI expansion largely determines which L^2 functions are included in the wave function.

We employ the diatomic version of the UK molecular R-matrix codes [9] which uses Slater type orbitals (STOs) to represent the target, and numerical orbitals in a partial wave expansion to represent the continuum [10]. The approach necessitates the use of a Buttle [11] correction to allow for the arbitrary fixed boundary conditions imposed on the continuum basis orbitals.

2.2 The BeH^+ target

We use a CI representation of the target. As is well known, the choice of basis sets play a vital role in the quality of such calculations. Several STO basis sets, namely those of Cade and Huo [12], Ema et al. [13] and of Bagus et al. [14] were tested and finally, the STO basis sets of Bagus et al. [14] were chosen as these gave target excitation energies closest to those of MRSDCI calculation [5] and of Bishop and Cheung [3]. Moreover, with these basis sets our excitation energies for the bound states were also in very close agreement with the calculations of Pitarch-Ruiz et al. [15], Petsalakis et al. [16] and Bruna et al. [17] (see Tab. 3). These basis sets contain 5 s-type, 4 p-type, 2 d-type and 1 f-type STOs centered on the Be atom and 3 s-type, 1 p-type and 1 d-type STOs centered on the H atom respectively. The STOs were used to build a basis of 31 molecular orbitals containing 17σ, 9π, 4δ and 1ϕ orbitals. An initial SCF calculation was performed for the lowest $^2\Sigma^+$ state of BeH^+ using these molecular orbitals. Finally 17σ, 9π and 4δ $^2\Sigma^+$ SCF molecular orbitals were used in a CI calculation. We tested several target models. Of these the model selected, namely $(1\sigma)^2$ (2σ-6σ, 1π, $2\pi)^2$, had the 1σ orbitals frozen and the complete active space (CAS) spanning the valence orbitals was defined by (2σ-6σ, 1π, $2\pi)^2$. This model was chosen as it gave the best target energies.

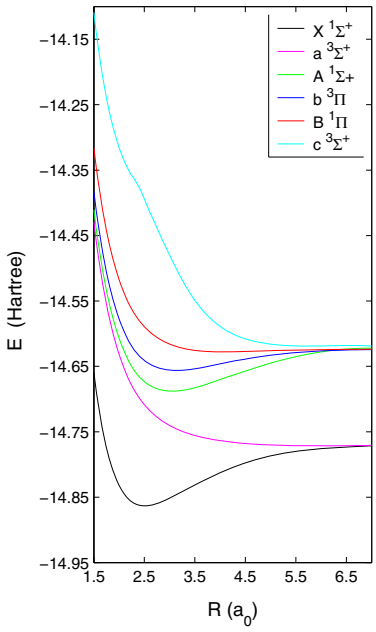

Fig. 1. (Color online) Potential energy curves for the lowest 6 states of the BeH^+ molecule.

Figure 1 shows the behaviour of the lowest six singlet and triplet states of BeH^+ used in our work as a function of the bond length.

All calculations reported here are performed at the BeH equilibrium bond length $R_e = 2.5369a_0$. The excitation energies for the singlet and triplet states of BeH^+ used in this work are summarized in Table 1. These are compared with the values given by Machado and Ornellas [5] and those of Bishop and Cheung [3] wherever available, and we find our excitation energies to be within 0.5 eV of these data. Note however, that the energies of Machado and Ornellas [5] and that of Bishop and Cheung [3] are presented at $R = 2.5a_0$ (obtainable from Machado and Ornellas [5]) whereas ours are at $R = R_e = 2.5369a_0$.

We have used 8 (6σ and 2π) BeH^+ SCF orbitals in the scattering calculation. These were supplemented by continuum orbitals F_{ij} obtained as a truncated partial wave expansion around the center of mass. Only partial waves with $l \leq 6$ and $m \leq 2$ were retained in the calculation. The radial parts of the continuum functions were generated as numerical solutions of an isotropic Coulomb potential. Those solutions with an energy below 10 Ryd were retained. This process produced 175 (70σ, 58π, 47δ) continuum functions which were then Schmidt orthogonalized to the target SCF orbitals.

Even here, we tested several scattering models. Finally we chose the model which used a $(1\sigma$-6σ, 1π, $2\pi)^4$ CAS target wave function, as this gave the best vertical excitation energies for the BeH bound states compared to other works. Scattering calculations were then performed using this model, for BeH states with $^2\Sigma^+$, $^2\Sigma^-$, $^2\Pi$, $^2\Delta$, $^4\Sigma^+$, $^4\Sigma^-$, $^4\Pi$ and $^4\Delta$ total symmetries. The summary of different target states used for each symmetry in the close-coupling expansion of the electron wave function in

Table 1. Ground state energies (in Hartree) and vertical excitation energies (in eV) of the BeH^+ molecule at $R_e = 2.5369a_0$. $N(\Gamma)$ is the number CSF's generated for each symmetry.

Excited state	Present	MRSDCI[a]	Bishop and Cheung[b]
$N(^1\Sigma^+)$	**190**		
X $^1\Sigma^+$	−14.86328	−14.93710	−14.93343
A $^1\Sigma^+$	5.11	5.27	5.48
$^1\Sigma^+$	13.69		
$N(^1\Sigma^-)$	**69**		
$^1\Sigma^-$	27.25		
$N(^1\Pi)$	**188**		
B $^1\Pi$	7.37	7.32	
$^1\Pi$	14.87		
$^1\Pi$	21.04		
$N(^1\Delta)$	**82**		
$^1\Delta$	20.40		
$N(^3\Sigma^+)$	**189**		
a $^3\Sigma^+$	4.12	4.31	
c $^3\Sigma^+$	12.57	12.03	
$^3\Sigma^+$	13.09		
$^3\Sigma^+$	14.75		
$N(^3\Sigma^-)$	**127**		
$^3\Sigma^-$	19.27		
$^3\Sigma^-$	28.02		
$^3\Sigma^-$	38.47		
$N(^3\Pi)$	**240**		
b $^3\Pi$	5.99	6.21	
$^3\Pi$	14.56		
$^3\Pi$	17.60		
$^3\Pi$	24.46		
$N(^3\Delta)$	**85**		
$^3\Delta$	27.51		

[a] Machado and Ornellas [5]; vertical excitation energies calculated at $R = 2.5a_0$.
[b] Bishop and Cheung [3]; vertical excitation energies calculated at $R = 2.5a_0$.

Table 2. Number and symmetry of target states used in the close-coupling expansion equation (1), as a function of total symmetry. The lowest energy target state of each symmetry was used in each case.

Symmetry	Number	Target states used
$^2\Sigma^+$	9	three $^1\Sigma^+$ and $^3\Sigma^+$, two $^1\Pi$ states and one $^3\Pi$.
$^2\Pi$	9	as for $^2\Sigma^+$.
$^2\Sigma^-$	9	two $^1\Sigma^-$ states, three $^1\Pi$ and $^3\Pi$ states, one $^1\Delta$ states.
$^2\Delta$	8	three $^1\Sigma^+$ and $^3\Sigma^+$ states, one $^1\Pi$ state and one $^3\Pi$ state.
$^4\Sigma^+$	6	three $^3\Sigma^+$ and $^3\Pi$ states.
$^4\Pi$	8	four $^3\Sigma^+$ states, three $^3\Pi$ states and one $^3\Sigma^-$ state.
$^4\Sigma^-$	8	three $^3\Sigma^-$ states, four $^3\Pi$ states and one $^3\Delta$ state.
$^4\Delta$	8	three $^3\Sigma^+$ and $^3\Pi$ states and two $^3\Sigma^-$ states.

equation (1) is presented in Table 2. At this stage all calculations were performed within the standard adiabatic nuclei approximation [18].

3 Results

In the following subsections we present our calculation of bound states of BeH, cross sections for electronic excitation, cross sections for rotational excitation and resonance positions and widths at $R_e = 2.5369a_0$. A more complete study and discussion on the resonances will be presented in a subsequent paper. To the best of our knowledge there are no previous works on these cross sections and hence we do not have any data, experimental or theoretical, to compare with.

3.1 Bound states

To test the validity and the quality of our scattering model, we calculated the bound states and their quantum defects at $R_e = 2.5369a_0$. We propose to give in detail

Table 3. Vertical excitation energies (in eV) from the $^2\Sigma^+$ ground state of the BeH molecule at $R_e = 2.5369a_0$.

Excited state	This work	FCI[a]	MRD-CI[b]	MRD-CI[c]
X $^2\Sigma^+$	0.0	0.0	0.0	0.0
1 $^2\Pi$	2.46	2.53	2.56	2.51
2 $^2\Sigma^+$	5.44	5.52	5.61	5.51
3 $^2\Sigma^+$	5.47	5.66	5.51	5.56
4 $^2\Sigma^+$	6.02	6.12	6.12	6.12
2 $^2\Pi$	6.23	6.30	6.31	6.42
5 $^2\Sigma^+$	6.59	6.72	6.71	6.81
3 $^2\Pi$	6.57	6.72	6.74	6.86
1 $^2\Delta$	6.64	6.73	6.77	6.96
6 $^2\Sigma^+$	6.90	7.00		
7 $^2\Sigma^+$	7.06	7.18		
4 $^2\Pi$	7.15	7.26	7.27	
5 $^2\Pi$	7.36	7.36		
8 $^2\Sigma^+$	7.29	7.40		
2 $^2\Delta$	7.33	7.42		
9 $^2\Sigma^+$	7.46	7.54		
6 $^2\Pi$	7.46	7.58		7.57
1 $^2\Sigma^-$	9.16	8.19†		
1 $^4\Pi$	5.16	5.84		5.82

[a] Pitarch-Ruiz et al. [15]; vertical excitation energies calculated at 1.3269 Å $= 2.5075a_0$.
[b] Petsalakis et al. [16]; vertical excitation energies calculated at 1.346 Å $= 2.5436a_0$.
[c] Bruna and Grein [17]; vertical excitation energies calculated at 1.3426 Å $= 2.5371a_0$.
† T_e value (see text), quoted from Pitarch-Ruiz et al. [23].

the bound state potential energy (PE) curves for the BeH states in a later work.

For the scattering calculation, the inner region solutions obtained were used to construct an R-matrix on the boundary. In the outer region, in addition to the Coulomb potential, the potential was given by the diagonal and off-diagonal dipole and quadrupole moments of the BeH^+ target states. To find bound states, asymptotic outer region wave functions were constructed using a Gailitis expansion [19] and then integrated inwards to the R-matrix boundary. For the present work the R-matrices were propagated to $50a_0$ and an improved Runge-Kutta-Nystrom procedure implemented by Zhang et al. [20] was used. Bound states were then found using the searching algorithm of Sarpal et al. [21] with the improved nonlinear, quantum defect based grid of Rabadán and Tennyson [22].

Table 3 presents the vertical excitation energies from the $X\ ^2\Sigma^+$ ground state of BeH. Our results are compared with the vertical excitation energies from the FCI calculation of Pitarch-Ruiz et al. [15], the MRD-CI calculation of Petsalakis et al. [16], and the MRD-CI calculation of Bruna and Grein [17]. We find good agreement with all the other works and, except for the 1 $^4\Pi$ and the lowest $^2\Sigma^-$ states, our excitation energies are within 0.5 eV of the others. For the lowest $^2\Sigma^-$ state, the vertical excitation energy was compared with the adiabatic T_e value given by Pitarch-Ruiz et al. [23] as no other work was available to compare with. The T_e value is the energy difference between an excited state (here $^2\Sigma^-$) at the calculated minimum and the ground state at its equilibrium geometry. Our vertical excitation energy for this state lies within about 1 eV of their T_e value.

We also present in Table 4 the quantum defects for some of the Rydberg states of BeH. These are compared with the quantum defects given by Pitarch-Ruiz et al. [15] and are generally in good agreement with them. An important factor in comparing these quantum defects is the vertical ionisation potential. Our calculation gives an ionisation potential (IP), or binding energy for the ground X $^2\Sigma^+$ state of BeH of 8.214 eV. This agrees very well with the experimental value of Colin et al. [24] who obtained 8.195 ± 0.062 eV. Previous theoretical estimates are slightly higher than this: Pitarch-Ruiz et al. [15] obtained a vertical IP of 8.298 eV while Bruna and Grein [17] obtained 8.33 eV.

3.2 Resonance positions and widths

A feature of low-energy scattering from a cation is the occurrence of series of resonances that can be characterized by a position and width or, alternatively, with a complex quantum defect. These resonances manifest themselves as sharp structures in the fixed-nuclei cross sections and provide the standard route to break-up of molecular ions via dissociative recombination. Table 5 presents calculation of resonance positions, widths and their effective quantum numbers for BeH at its equilibrium bond length of $R = 2.5369a_0$ for the doublet states. Resonances are presented in separate regions defined by the excitation threshold of the lowest electronically excited states of BeH^+. The effective quantum numbers are calculated assuming the resonance can be associated with the excited state directly above. However it is clear that while some effective quantum numbers and hence resonances fall neatly into series characterized by similar quantum defects, others do not. This behaviour is caused by so-called intruder states where the resonance is associated with a higher electronic state.

The behaviour of these intruder states, and indeed the curves necessary for dissociative recombination, are best characterized by studying the behaviour of the resonances as function of bond length. We are currently working on this.

3.3 Electronic excitation

Figure 2 shows excitation cross sections from the ground state to the first four excited states of BeH^+, namely the a $^3\Sigma^+$, A $^1\Sigma^+$, b $^3\Pi$ and the B $^1\Pi$ states. The cross sections are quite significant and show resonance structures, as is to be expected for fixed nuclei calculations.

The a $^3\Sigma^+$ is dissociative so that our excitation cross section actually corresponds to the electron impact dissociation cross section to $Be^+ + H$. As shown in Figure 1, the other electronic states are associated with an excited asymptote corresponding to $Be + H^+$. Above the energy where this asymptote is open, i.e. above 6.57 eV, the other

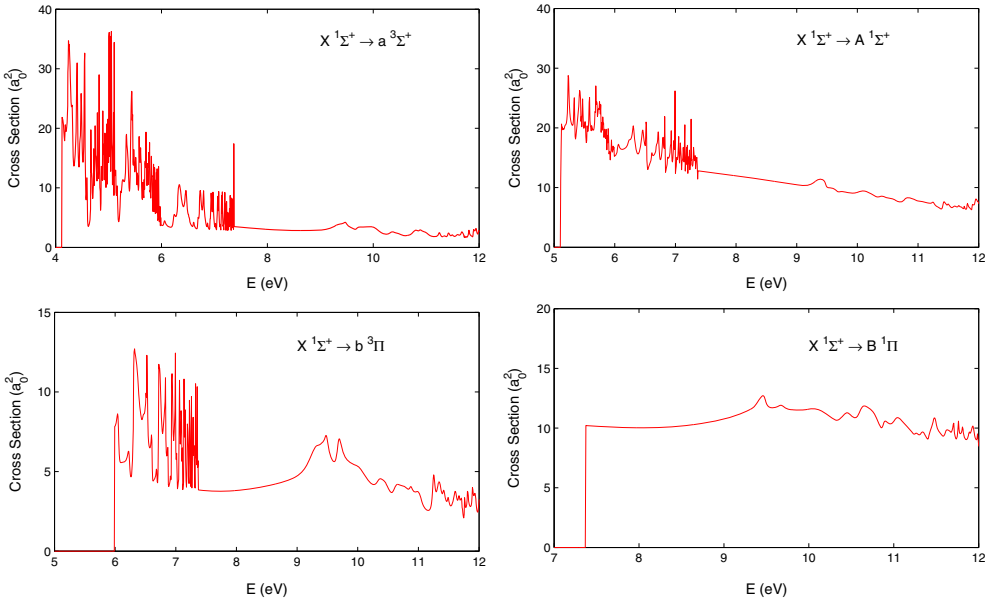

Fig. 2. (Color online) Excitation cross sections from the X $^2\Sigma^+$ ground state of the BeH^+ molecule to the excited states indicated in each panel at $R = 2.5369a_0$.

Table 4. Quantum defects of some Rydberg states of BeH at $R_e = 2.5369a_0$.

State	This work	FCI[a]	State	This work	FCI[a]	State	This work	FCI[a]
s-type								
2 $^2\Sigma^+$ (3*s*)	0.789	0.787						
6 $^2\Sigma^+$ (4*s*)	0.791	0.762						
9 $^2\Sigma^+$ (5*s*)	0.786	0.763						
p-type								
4 $^2\Sigma^+$ (3*p*)	0.521	0.501	2 $^2\Pi$ (3*p*)	0.383	0.390			
7 $^2\Sigma^+$ (4*p*)	0.581	0.511	4 $^2\Pi$ (4*p*)	0.440	0.380			
d-type								
5 $^2\Sigma^+$ (3*d*)	0.114	0.064	3 $^2\Pi$ (3*d*)	0.131	0.064	1 $^2\Delta$ (3*d*)	0.071	0.054
8 $^2\Sigma^+$ (4*d*)	0.178	0.108	5 $^2\Pi$ (4*d*)	0.011	0.191	2 $^2\Delta$ (4*d*)	0.086	0.063

[a] Pitarch-Ruiz et al. [15].

excitation cross sections give an estimate for electron impact dissociation to the Be + H^+ channel.

3.4 Rotational excitation

Figure 3 presents cross sections for the rotational excitations corresponding to the transitions $j = 0 \rightarrow 1$, $j = 0 \rightarrow 2$ and $j = 0 \rightarrow 3$. The geometry was frozen at BeH^+ equilibrium bond length $R = 2.5369a_0$ which gives a dipole moment of 2.7266 Debye. The cross sections were calculated using the ROTIONS program of Rabadán and Tennyson [25]. Excitation cross sections obtained from the T-matrix calculated above were supplemented by the dipole Coulomb-Born cross section [26] to include the contributions due to high-l partial waves. Excitations greater $\Delta j = 3$ are negligible and therefore not considered. The adiabatic nuclear approximation used in these calculations considers all rotational states to be degenerate. We have cut the cross sections so they are zero below the excitation threshold but take the calculated value above. This

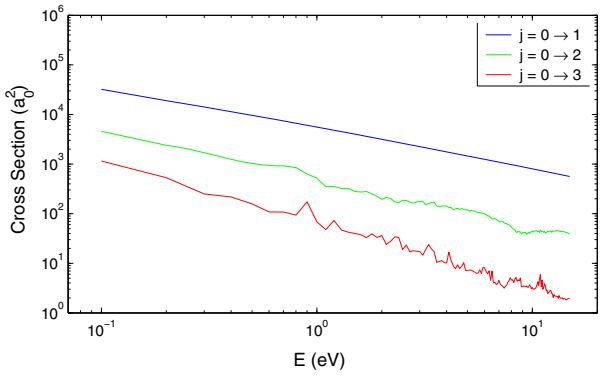

Fig. 3. (Color online) BeH^+ rotational excitation cross sections.

simple treatment of threshold effects was found to give excellent agreement with treatments that explicitly include allowance for the excitation threshold [27]. As has been found before for molecular ions with large dipole

Table 5. Resonance positions and widths (in Ryd) and effective quantum numbers at $R = 2.5369a_0$ for doublet states of the e-BeH^+ system below the first two BeH^+ excited states. Numbers within brackets indicate power of 10.

Below $a\ ^3\Sigma^+$ state			Below $A\ ^1\Sigma^+$ state		
Position	Width	ν	Position	Width	ν
$^2\Sigma^+$					
0.0792	0.9930(–02)	2.1154	0.3131	0.3951(–03)	4.0063
0.1523	0.1003(–01)	2.5795	0.3174	0.2149(–02)	4.1522
0.1679	0.3572(–02)	2.7249	0.3235	0.3460(–02)	4.3894
0.1903	0.2612(–02)	2.9840	0.3275	0.1125(–02)	4.5683
0.2067	0.3263(–02)	3.2288	0.3291	0.3852(–02)	4.6466
0.2230	0.1181(–02)	3.5446	0.3378	0.1030(–02)	5.1531
0.2302	0.2366(–02)	3.7152	0.3490	0.6249(–03)	6.1518
0.2349	0.4561(–03)	3.8430	0.3521	0.3923(–03)	6.5506
0.2411	0.8913(–03)	4.0303			
0.2484	0.1957(–02)	4.2937			
$^2\Pi$					
0.1591	0.1554(–02)	2.6395	0.3130	0.3622(–03)	4.0029
0.1864	0.1075(–03)	2.9338	0.3239	0.1515(–02)	4.4059
0.2195	0.2131(–02)	3.4685	0.3296	0.1649(–02)	4.6718
0.2267	0.1344(–02)	3.6289	0.3431	0.3103(–03)	5.5637
0.2372	0.1430(–03)	3.9096	0.3464	0.8235(–03)	5.8740
0.2414	0.8768(–04)	4.0428	0.3520	0.2130(–03)	6.5415
0.2475	0.4538(–02)	4.2584	0.3577	0.3923(–03)	7.5068
0.2558	0.4389(–02)	4.6212			
0.2714	0.4626(–03)	5.6620			
0.2793	0.1374(–03)	6.5540			
$^2\Delta$					
0.0526	0.2402(–01)	1.9997	0.3072	0.1032(–02)	3.8275
0.1927	0.1688(–02)	3.0159	0.3127	0.3355(–03)	3.9926
0.2382	0.1743(–03)	3.9412	0.3268	0.8957(–02)	4.5333
0.2418	0.4265(–03)	4.0540			
0.2593	0.2975(–02)	4.8023			
0.2635	0.2466(–03)	5.0569			

moments [28], the rotational excitation cross section is dominated by $\Delta j = 1$ transitions at all energies. This transition is largely driven by the long-range dipole potential. Conversely the $\Delta j = 2$ and $\Delta j = 3$ transitions are determined by short-range interactions and are therefore sensitive to resonance effects, as can be seen by the structure in the cross sections for these transitions.

4 Conclusion

We have studied electron collisions with the BeH^+ molecule using the R-Matrix method. Bound state energies and quantum defects for the BeH states at $R_e = 2.5369a_0$ are obtained and are in good agreement with other calculations.

Cross sections for excitations to the first four BeH^+ states are calculated. These can be used to estimate electron impact dissociation of BeH^+ with branching ratios to the two low-lying asymptotic channels: $Be^+ + H$ and $Be + H^+$. Below these electronic excitation thresholds, we also calculated cross sections for rotational excitation of BeH^+ with $\Delta j = 1, 2, 3$. To the best of our knowledge, all these data have been obtained for the first time.

We thank Ioan Schneider for helpful discussions about this work.

References

1. Culhum Centre for Fusion Energy news, New experimental campaign underway at JET (2011), http://www.ccfe.ac.uk/news_detail.aspx?id=128
2. F.R. Ornellas, J. Phys. B At. Mol. Phys. **15**, 1977 (1982)
3. D.M. Bishop, L.M. Cheung, J. Chem. Phys. **80**, 4341 (1984)
4. F.R. Ornellas, J. Chem. Phys. **82**, 379 (1985)
5. F.B.C. Machado, F.R. Ornellas, J. Chem. Phys. **94**, 7237 (1991)
6. P.G. Burke, *R-Matrix Theory of Atomic Collisions* (Springer, Berlin, 2011)
7. J. Tennyson, Phys. Rep. **491**, 29 (2010)
8. J. Tennyson, J. Phys. B At. Mol. Opt. Phys. **29**, 6185 (1996)
9. L.A. Morgan, J. Tennyson, C.J. Gillan, Comput. Phys. Commun. **114**, 120 (1998)
10. J. Tennyson, L.A. Morgan, Phil. Trans. R. Soc. Lond. A **357**, 1161 (1999)
11. P.J.A. Buttle, Phys. Rev. **160**, 719 (1967)
12. P.E. Cade, W.M. Huo, J. Chem. Phys. **47**, 614 (1967)

13. I. Ema, J.M. García De La Vega, G. Ramírez, R. López, J. Fernández Rico, H. Meissner, J. Paldus, J. Comput. Chem. **24**, 859 (2003)
14. P.S. Bagus, C.M. Moser, P. Goethals, G. Verhaegen, J. Chem. Phys. **58**, 1886 (1973)
15. J. Pitarch-Ruiz, J. Sánchez-Marín, A.M. Valesco, J. Comput. Chem. **29**, 523 (2007)
16. I.D. Petsalakis, G. Theodorakopoulos, C.A. Nicolaides, J. Chem. Phys. **97**, 7623 (1992)
17. P.J. Bruna, F. Grein, Phys. Chem. Chem. Phys. **5**, 3140 (2003)
18. D.M. Chase, Phys. Rev. **104**, 838 (1956)
19. C.J. Noble, R.K. Nesbet, Comput. Phys. Commun. **33**, 399 (1984)
20. R. Zhang, K.L. Baluja, J. Franz, J. Tennyson, J. Phys. B At. Mol. Opt. Phys. **44**, 035203 (2011)
21. B.K. Sarpal, S.E. Branchett, J. Tennyson, L.A. Morgan, J. Phys. B At. Mol. Opt. Phys. **24**, 3685 (1991)
22. I. Rabadán, J. Tennyson, J. Phys. B At. Mol. Opt. Phys. **29**, 3747 (1996)
23. J. Pitarch-Ruiz, J. Sánchez-Marín, A.M. Valesco, I. Martin, J. Chem. Phys. **129**, 054310 (2008)
24. R. Colin, D. De Greef, P. Goethals, G. Verhaegen, Chem. Phys. Lett. **25**, 70 (1974)
25. I. Rabadán, J. Tennyson, Comput. Phys. Commun. **114**, 129 (1998)
26. S.I. Chu, A. Dalgarno, Phys. Rev. **10**, 788 (1974)
27. A. Faure, V. Kokoouline, C.H. Greene, J. Tennyson, J. Phys. B At. Mol. Phys. **39**, 4261 (2006)
28. A. Faure, J. Tennyson, Mon. Not. R. Astron. Soc. **325**, 443 (2001)